Revista Mexicana de Física S **58** (2) 19–23 DICIEMBRE 2012

Hydrothermal synthesis, magnetic susceptibility, electrical transport and vibrational order of the polycrystalline structure $La_{0.5}Ba_{0.5}MnO_3$

J. Jativa, J.F. Jurado, and C. Vargas-Hernandez
Laboratorio Propiedades Ópticas de Materiales, Universidad Nacional de Colombia, A.A 127, Manizales, Colombia.
e-mail: jajativah@unal.edu.co

Recibido el 25 de junio de 2010; aceptado el 18 de octubre de 2010

The $La_{0.5}Ba_{0.5}MnO_3$ (LBMO) polycrystalline compound was sintered by hydrothermal technique [1,2]. The precursors were dissolved in deionized water using potassium hydroxide (KOH) as mineralizer and taken to an environment of high pressure with a temperature of 240°C for 24 hours. The product is calcined in a furnace at 1000°C for 24 hours at atmospheric pressure. The XRD patterns at room temperature shows a cubic crystal structure with a lattice parameter of a = 3.910 ± 0,001Å and a crystallite size of 73 nm, these values were obtained by the method of Cohen with a Gaussian fit. The conductivity measurements show a increase as the temperature increases following a type-insulating behavior for the temperature range 270 a 500 K in vacuum.
The increase of conductivity with temperature, thermally activated behavior in the system is attributed to the generation of oxygen vacancies, this particular case is mainly attributed to the facilitation of electrons e_g exchange between ions Mn^{3+} and Mn^{4+}. The susceptibility AC as a function of temperature showed a transition from ferromagnetic-paramagnetic phase with a transition temperature about 356 K. The change of the imaginary part of the susceptibility at this temperature is indicative of the Hund exchange effect for electrons t_{2g} as the temperature increases and approaches the critical temperature.
Micro-Raman measurements at room temperature showed the presence of active modes associated with rotational vibration, octahedral inflection, stretching in phase and symmetric stretching of the octahedral's basal oxygen MnO_6 in 271, 415, 566, and 643 cm-1, respectively.

Keywords: Manganites; magnetic properties; AC susceptibility; micro-Raman.

El compuesto $La_{0.5}Ba_{0.5}MnO_3$ (LBMO) policristalino fue sinterizado por la técnica hidrotermal [1,2]. Los precursores son disueltos en agua desionizada utilizando hidróxido de potasio (KOH) como mineralizador y fueron llevados a un ambiente de alta presión con temperatura alrededor de 240^{o}C por 24 horas. El producto se calcina a 1000°C por 24 horas, a presión atmosférica. Los difractogramas de rayos-X a temperatura ambiente, revelaron que el material cristaliza con estructura cubica, cuyo parámetro de red a = 3.910 ± 0,001Å y tamaño de cristalito 73 nm. Estos valores fueron obtenidos por el método de Cohen y ajuste Gaussiano. La conductividad del LBMO aumenta a medida que la temperatura aumenta siguiendo un comportamiento tipo-aislante, para el intervalo de temperaturas de 270 a 500 K en vació. El incremento de la conductividad térmicamente activado, es atribuido a la generación de vacancias de oxigeno, que de alguna forma presenta un favorecimiento en el intercambio de electrones e_g entre los iones Mn^{3+} y Mn^{4+}. La susceptibilidad AC en función de la temperatura mostró una transición de fase ferromagnética-paramagnética con temperatura de transición cercana a 356 K. El cambio presentado por la parte imaginaria de la susceptibilidad a esta temperatura, es un indicativo del efecto de intercambio tipo Hund para los electrones t_{2g} a medida que la temperatura aumenta. Medidas micro-Raman a temperatura ambiente mostraron la presencia de los modos activos asociados con las vibraciones de rotación, inflexión de los octaedros, estiramientos en fase y estiramientos simétricos de los oxígenos basales de los octaedros MnO_6 en: 271, 415, 566, y 643 cm^{-1}, respectivamente.

Descriptores: Manganitas; propiedades magnéticas; susceptibilidad AC.; micro-Raman.

PACS: 61.05.cp; 75.50.-y.

1. Introduction

The manganese oxides with mixed valence with $La_{1-x}A_xMnO_3$ generic formula are of great interest both in basic and applied level in particular for presenting magnetoresistive effect near the Curie temperature (Tc), this effect is attributed mainly to the double exchange effect [3,4]. The magnetic and transport properties are determined largely by the ion concentration relation Mn^{3+}/Mn^{4+}. This relation can vary strongly by the alkaline divalent elements substitution (Ca^{2+}, Sr^{2+}, Ba^{2+}, between others) in the ion A position, and the vacancies formation in the metal subnets and / or the oxygen stoichiometry.

In the manganese oxides sintering, other important factors to consider are the pioneers and the used techniques to obtain them, since they may substantially affect: The microscopic agglomeration, homogeneity, crystallinity, between other parameters. In view of these arguments, it has been implemented a variety of sintering methods. The most usual is called solid state reaction at high temperatures, which requires: oxides, carbonates or nitrates with sintering temperatures above 1000°C [5]. The shortcoming of this technique is mainly the difficulty of controlling the oxygen content. Another methodology is called sol-gel, in this are executed complexation processes and precursors' dissolution, processes that are not easy to control. In view of these arguments, we have decided to sinter the $La_{0.5}Ba_{0.5}MnO_3$ compound using the methodology called hydrothermal, following the made arguments in Refs. 6 and 7. The process is based on using oxides, nitrates and hydroxides locked in an autoclave. This methodology presents an attractive synthesis of complex ox-

ides using autogenous pressures and maximum temperatures near 300°C increasing the reaction between the precursors.

2. Experimental data

The $La_{0.5}Ba_{0.5}MnO_3$ compound is obtained from available precursors: $KMnO_4$ (99.0% Panreac), $MnCl_24H_2O$ (99.0% Riedel-de Haën), $La(NO_3)_36H_2O$ (99.9% Merck), $BaCl_22H_2O$ (99.0% Scharlau) and KOH (90.0% CarloErba), mixed in a cylindrical Teflon body immersed in an autoclave (stainless steel). The precursors were weighed stoichiometrically with molar ratio of 0.6M $KMnO_4$, 1.2M $MnCl_24H_2O$, 3.1M $La(NO_3)_36H_2O$, 1.6M $BaCl_22H_2O$. These are mixed independently in deionized water at room temperature, then, are mixed in a single container with KOH to adjust the alkalinity solution in about 10. The compound is stirred for one hour. The reaction equation of mass balance is given by:

$$\begin{aligned} &La(NO_3)_3.6H_2O + BaCl_2.2H_2O + 3.6KMnO_4 \\ &+ 0.7MnCl_2.4H_2O + 7.2KOH \Rightarrow 2La_{0.5}Ba_{0.5}MnO_3 \\ &+ 3KNO_3 + 4.8KCl + 17.2H_2O \end{aligned} \quad (1)$$

The product is poured into the Teflon container with a filling factor of 60%, this is set in an autoclave and heated to 240°C for 24 hours. The final compound is washed with distilled water several times, finally dried at 80°C. The product (brown powder) is carried to a furnace and heated to a series of ramps up to the final temperature of 1000°C.

The X-ray diffractograms at room temperature are performed with a D8 Advance (Broker AXS) to sweep angle between $20° < 2\theta < 70°$, 0.020° steps and 5.0 s / step exposure. The AC magnetic susceptibility is measured using the "Lock-in" technique for the range temperatures of 270 and 500 K. The resistivity measurements were carried out with the method of the four points above the atmosphere. Micro-Raman measurements were carried out with a LabRam HR800 Ramanequipment of the Ywom Horiba Jobin commercial house.

3. Analysis and results

Figure 1 shows the diffractogram for the $La_{0.5}Ba_{0.5}MnO_3$ compound at room temperature. The position and relative intensity of main peaks reveal the presence of a cubic crystal structure with parameter a=3.910±0,001Å. This value was calculated by the Cohen method for a Gaussian fit. These results concur with those reported by Ping Chai [2] and correspond to the determined values for obtained compounds following other sintering methods [7,8]. The crystallite size was calculated using the Debye-Scherrer formula:

$$t = \frac{k.\lambda}{\beta.\cos\theta} \quad (2)$$

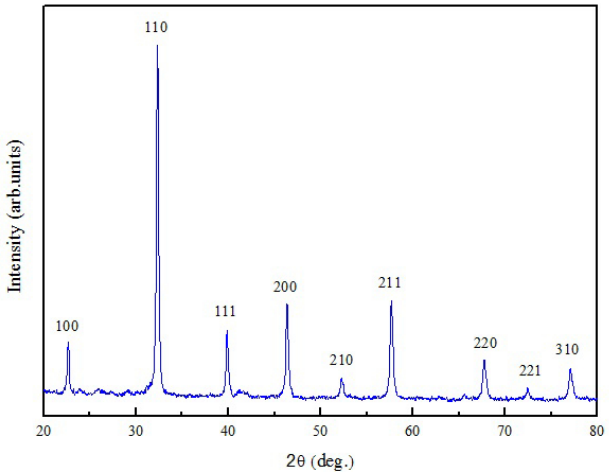

FIGURE 1. X-ray diffraction at room temperature for $La_{0.5}Ba_{0.5}MnO_3$. Miller indices are assigned to a cubic structure.

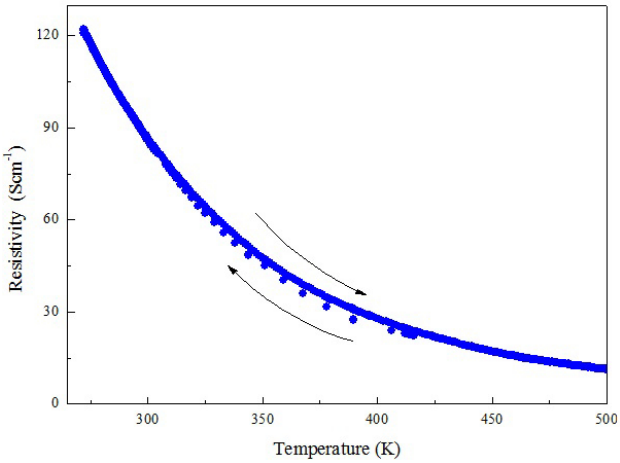

FIGURE 2. Resistivity variation with the temperature for LBMO. The arrows indicate the direction of heating or cooling.

where k is the normalization factor (0.9), λ the wavelength (CuKα, λ = 1.54060 A), β is the half width of the peak and θ is the Bragg angle. The peaks individual analysis with Gaussian refinement, threw a crystallite size of 73 nm, value that is consistent with the reported in Ref. 8.

From these results, we can say that the $La_{0.5}Ba_{0.5}MnO_3$ compound, obtained by hydrothermal method shows good crystalline quality. The acceptable crystal quality can be attributed to the heat treatment and to the KOH mineralizer used in the methodology, since it favors the crystallization and promotes the compounds dissolution and the desired phase formation [9,10,11].

Figure 2 shows as the resistivity decreases as temperature increases following a type-insulating behavior and thermally activated at $T > Tc$. The material's conductivity increase with the temperature is attributed to the oxygen vacancies generation, an effect that contributes to the eg electron exchange furthering between Mn^{3+} y Mn^{4+}[12,13,14] ions.

TABLE I. Raman modes experimental values for several compounds perovskite type.

Mode	$La_{0.5}Ba_{0.5}MnO_3$ Hydrothermal Route	$BaMnO_3$ Ref 20	$La_{1-x}Ba_xMnO_3$ $0.05 \leq x \leq 1$ Ref 19	$LaMnO_3$ Ref 17	(La,Pr)MnO_3 Ref 21	$CaMnO_3$ Ref 18
$A_g(2) - B_{1g}(3)$	271			275, 220	290	278
Ag(3)	414	415	415			
$A_g(2) - B_{3g}(2)$	566	560	556			
$B_{2g}(2)$	643	642				

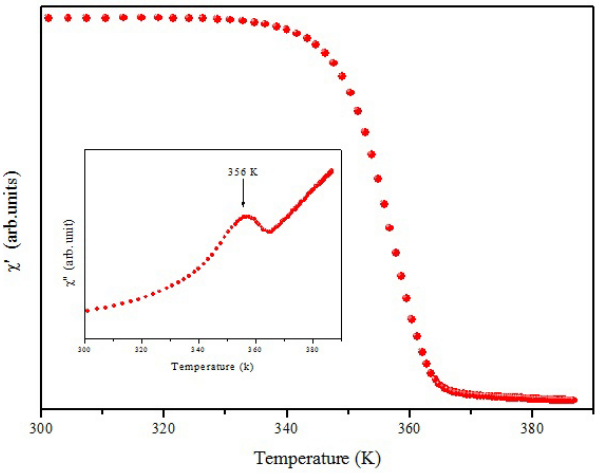

FIGURE 3. Real part of AC susceptibility, depending on the $La_{0.5}Ba_{0.5}MnO_3$ temperature, for a frequency of 95 kHz. The inset shows the AC susceptibility imaginary part. The transition temperature *Tc* = 356 K

AC susceptibility (Fig. 3) shows the $La_{0.5}Ba_{0.5}MnO_3$ magnetic state in the temperature function, where the components: real and imaginary part reflects the magnetic dynamic of the material, and the presence of a ferromagnetic-paramagnetic transition phase with transition temperature close to Tc=356 K, with the presence of the peak in the imaginary part (inset Fig. 3). In Ref. 15 is reported transition temperature near 330 K as crystals for this compound, while for the obtained powder material by the sol-gel method the temperature is about 351.7 K [16]. This transition phase is associated with the double exchange effect, which involves the e_g electrons movement between Mn closer sites with different valence through the ligation oxygen. That is to say, the states' degeneracy involved in the links $Mn^{3+}-O^{2-}-Mn^{4+}$ y $Mn^{4+}-O^{2-}-Mn^{3+}$ allow the e_g electron simultaneous transfer causing a net load change. As is well known that the exchange process electron spin is preserved with the addition to the Hund strong interaction in the double transfer is given as long as the t_{2g} spins present a ferromagnetic order.

Figure 4 shows $La_{0.5}Ba_{0.5}MnO_3$ micro-Raman spectrum at room temperature. The record shows the presence of allowed bands, which are compared with the reports presented in the literature for different perovskites. The bands are located at: 271, 414, 566 and 643 cm^{-1}, respectively. The band located at 271 cm^{-1} is called $B_{1g}(3)$ according to Ref. 17

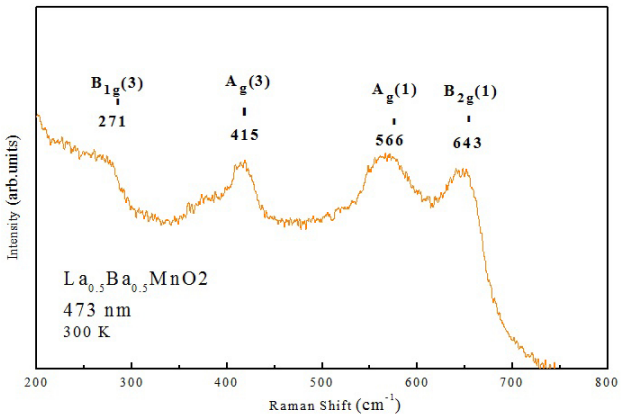

FIGURE 4. $La_{0.5}Ba_{0.5}MnO_3$ Micro-Raman spectrum compound at room temperature.

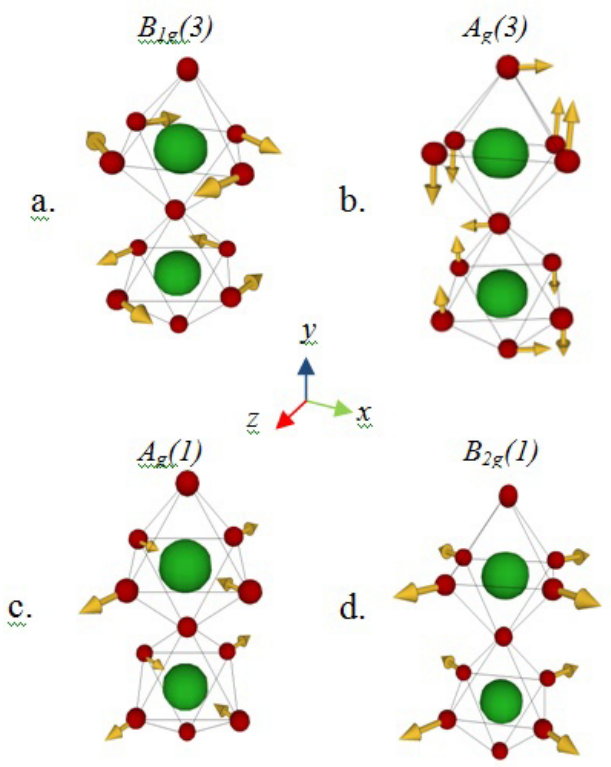

FIGURE 5. Raman modes allowed for $La_{0.5}Ba_{0.5}MnO_3$ as Ref 17.

and is associated with the oscillations out of phase MnO_6 octahedra along an axis (see Fig. 5a). Other authors [18] assign this band as $A_g(2)$, except that the octahedra oscillate in phase. The band located at 414 cm^{-1} corresponds to modes called $A_g(3)$, which involve a mismatch turning MnO_6 octahedra (see Fig. 5b). The band located at 566 cm^{-1} is associated with known modes with $A_g(2)$ and corresponds to a mode of type "breathing" and accompanied by a MnO_6 octahedra symmetrical distortion around Mn, in these circumstances Mn-O bonds are stretched while contracting in the *xz* plane in phase (see Fig. 5c). Some authors assign this band as $B_{3g}(2)$ mode [19]. The band located around 643 cm^{-1} corresponding to the denominated $B_{2g}(2)$ mode, this mode involves expansion processes and contraction in the basal oxygen phase, producing a stretching and compression of the Mn-O bonds in the plane *zx* (see Fig. 5d). Table I shows the comparison of active modes present in different manganites.

On the other hand, $B_{1g}(3)$, $A_g(3)$ and A_g (2) modes are also associated with Jahn-Teller distortion that can occur in the compound, and the present vibrational changes that are made by variations in the angles and distances presented, given by the (Ba^{2+}/La^{3+}) doping.

4. Conclusions

The methodology called hydrothermal route speeds up chemical reactions to obtain the manganite with good quality: crystalline, magnetic, transport and vibrational order. The $La_{0.5}Ba_{0.5}MnO_3$ compound showed a ferromagnetic-paramagnetic phase transition near Tc=365 K. This transition is correlated to the double exchange effect between Mn^{3+} and Mn^{4+} ions, showing a strong correlation with the load's transport. The manganite showed a good response about the vibrational order and allowed the comparison with present modes in other type of perovskites reported in the literature. The Raman active modes presence, are associated with the vibrations of: rotation and octahedra turning, as well as the symmetric stretching and of the octahedra's basal oxygen phase.

Acknowledgements

The authors thank the Laboratory of Chemistry of the National University of Colombia, Manizales by measurements of XRD.

1. S. Mirji, Y. Khollam, S. Deshpande, H. Potdar, R. Bathe, S. Sainkar, S. Date, *Materials, Microwave-hydrothermal accelerated solid state reaction route for the synthesis of* $La_{0.5}Ba_{0.5}MnO_3$, *Letters* **58** (2004) 837.
2. Chai P., Liu X., Wang Z., Lu M., Cao X. and Meng J., *Mechanism, and Magnetic Properties of* $La_{0.5}Ba_{0.5}MnO_3$, *Tunable Synthesis, Growth Crystal Growth & Design.* **7** (2007) 2568.
3. Inoue J., Maekawa S., *Spiral State and Giant Magnetorresistance in Perovskite Mn Oxides, Phys. Rev. Lett.* **74** (1995) 3407.
4. M. Salamon, *The physics of manganites: Structure and transport, Rev. Mod. Phys* **73** (2001) 583.
5. J. Jativa, E. Ortiz, J. Trochez, C. Vargas y J. Jurado, *Estudios Estructurales, Termogravimetría Magnética y Calorimetría en* $La_{0.5}Sr_{0.5}MnO_3$ *cerca de la Transición* PM-FM, RCF, **38** (2006) 1058.
6. S. Feng, and R. Xu, *New Materials in Hydrothermal Synthesis, Acc. Chem. Res* **34** (2001) 239.
7. J. Denga, L. Zhanga, H. Daia, H. Hea, C. Tong, *Hydrothermally fabricated single-crystalline strontium-substituted lanthanum manganite microcubes for the catalytic combustion of toluene, J. Mol. Catal. A: Chemical* 299 (2009) 60.
8. Yimin Cui, Liuwan Zhang, Chunchang Wang, Kai Shi, Bisong Cao, *Hydrogen annealing effects on polycrystalline* $La_{0.67}Ba_{0.33}MnO_3$ *compound, J. Magn. Mag. Mater.* **297** (2006) 21.
9. H. Wang, J. Liu, M. Zhu, B. Wang, and H. Yan, *Hydrothermal synthesis of strontium bismuth tantalate powder, Materials Letters* **57** (2003) 2371.
10. Malgorzata M. Lencka and Richard E. Riman, *Thermodynamics of the Hydrothermal Synthesis of Calcium Titanate with Reference to Other Alkaline-Earth Titanates, Chem. Mater.* **7** (1995) 18.
11. M. Traianidis, C. Courtois, A. Leriche, B. Thierry, *Hydrothermal Synthesis of Lead Zirconium Titanate (PZT) Powders and their Characteristics J. Eur. Ceram. Soc.* **19** (1999) 1023.
12. B. Raveau, C. Martin, A. Maignan, and M. Hervieu, *Insulator–metal like transition in air-synthesized* Mn^{4+}*-rich* $La_{1-x}Ba_xMnO_3$: *grain boundary phase effect B Phys. Condens. Matter* **14** (2002) 1297
13. R. Zainullina, N. Bebenin, V. Mashkautsan, V. Ustinov, Y. Mukovskii, *Hall effect and conductivity in* $La_{1-x}Ba_xMnO_3$ *single crystals, J. Magn. Mag. Mater.* **300** (2006) e137.
14. R.I. Bebenin, V.V. Zainullina, V.V. Mashkautsan, Ustinov and Ya.M. Mukovskii, *Electronic transport in ferromagnetic* $La_{1-x}Sr_xMnO_3$ *single-crystal manganites Phys. Rev. B* **69** (2004) 104.
15. J. Spooren, A. Rumplecker, F. Millange and R. Walton, *Subcritical Hydrothermal Synthesis of Perovskite Manganites: A Direct and Rapid Route to Complex Transition-Metal Oxides Chemistry of materials* **15** (2003) 1401
16. Jeffrey J. Urban, Lian Ouyang, Moon-Ho Jo, Dina S. Wang, and Hongkun Park., *Synthesis of Single-Crystalline* $La_{1-x}Ba_xMnO_3$ *Nanocubes with Adjustable Doping Levels, Nonoletters* **4** (2004) 1547.
17. M. Iliev, M. Abrashev and other, *Raman spectroscopy of orthorhombic perovskitelike* $YMnO_3$ *and* $LaMnO_3$, *Physical Review B* **57** (1998) 2872.
18. M. Abrashev, J. Backstrom, L. Borjesson, V. Popov, R. Chakalov, N. Kolev, R. Meng and M. Iliev, *Raman spectroscopy*

of $CaMnO_3$: Mode assignment and relationship between Raman line intensities and structural distortions, Physical Review B **65** (2002) 184301.

19. C. Roy and R. Budhani, *Raman, infrared and x-ray diffraction study of phase stability in* $La_{1-x}Ba_x$ MnO_3 *doped manganites, Journal of Applied physics* **85** (1998) 3124.

20. C. Roy, and R. Budhani, *Raman- and infrared-active phonons in hexagonal* $BaMnO_3$, *Physical Review B* **13** (1998) 58.

21. M. Carron and A. Andres, *Raman phonons and the Jahn–Teller transition in* $RMnO_3$ *manganites, J. Alloys. Compd.* **323-324** (2001) 417.